Temperature dependence of the Hall effect in pentacene field-effect transistors: Possibility of charge decoherence induced by molecular fluctuations

T. Uemura,[1,*] M. Yamagishi,[2] J. Soeda,[2] Y. Takatsuki,[2] Y. Okada,[2] Y. Nakazawa,[2] and J. Takeya[1,2,†]

[1]*The Institute of Scientific and Industrial Research, Osaka University, Ibaraki, Osaka 567-0047, Japan*

[2]*Graduate School of Science, Osaka University, Toyonaka, Osaka 560-0043, Japan*

(Received 28 April 2011; revised manuscript received 8 December 2011; published 17 January 2012)

Temperature dependence of the Hall effect is measured for both single-crystal and thin-film field-effect transistors of pentacene. At room temperature, the inverse Hall coefficient $1/R_H$ exceeds field-induced charge density Q by a factor of 2 at each gate-electric field for all the samples, regardless of their charge-carrier mobility and detailed subthreshold properties. Violating the band-transport model that $1/R_H$ equals to Q, the excess $1/R_H$ does not measure the charge amount anymore so that the result possibly indicates insufficient electromagnetic coupling due to somewhat reduced charge coherence. At lower temperatures, the deviation of $1/R_H$ from Q gradually diminishes to approach the band-transport behavior. Interestingly, the degree of the deviation has been universal for the measured five samples, including both polycrystal and single-crystal pentacene films. The result suggests that significant molecular fluctuation near room temperature can affect the fundamental electronic state.

DOI: 10.1103/PhysRevB.85.035313 PACS number(s): 72.80.Le, 71.20.Rv, 73.61.Ph

I. INTRODUCTION

Organic semiconductors, assemblies of weakly van der Waals bonded π-conjugated molecular units, render mechanically soft platforms, which enable moderate electronic charge transport. Since their weak bonding energy allows easy fabrication processes such as solution casting to form bendable electronic devices on plastic substrates near room temperature, they attract considerable attention with the expectation for the next-generation semiconductor industry of flexible and printable electronics. However, noting that both the weak molecular bonding and the freedom of molecular displacement are harmful for the intermolecular charge transfer, it is not simple to achieve high charge-transport efficiency and the mechanical flexibility simultaneously. It is required to understand the fundamental electronic state subjected to the intrinsic competition between the two.

Studies on charge transport in organic semiconductors date back to the 1970s, when both possibilities of band transport of diffusive electrons (described by wave numbers k's) and consecutive hopping processes between electronic states self-localized in the molecules (described by their positions r's) are already discussed.[1] Experimentally, however, a limited amount of charge-carrier density accessible with photodoping at that moment often caused significant difficulty to reach delocalized electronic states as the effects of charge-trapping sites are pronounced. Also, the crossover between the two extreme cases, in which either k or r describes the states properly, has never been detected experimentally without any measurement to deal with the one-electron phase coherence quantitatively.

With the development of high-performance organic field-effect transistors (OFETs), a much higher density of carriers up to 10^{20} cm^{-3} has been introduced in organic semiconductors, so that studies on intrinsic electronic states are accelerated with the measurement of steady current of the electrostatically doped high-mobility charge. In particular, development of organic single-crystal transistors contributed to detect genuine charge transport without influences of grain boundaries. Therefore, the nature of charge carriers in such systems has been intensively investigated by various methods.[2–4] Furthermore, recent measurements of Hall effect clearly showed that bandlike diffusive transport is realized at least in several high-mobility OFETs based on rubrene and dinaphtho[2,3-b:2′,3′-f]thieno[3,2-b]thiophene (DNTT) semiconductor layers; the experimental results for such devices satisfied the band-transport relation that $R_H = 1/Q$, where Q is the charge density precisely estimated from the dielectric capacitance of the gate-insulating layers.[5–8] The conclusion of the bandlike transport in rubrene single crystals was reinforced later by other experiments such as infrared spectroscopy and angle-resolved photoemission spectroscopy.[9,10]

The Hall voltage comes from the off-diagonal component σ_{xy} of the transport coefficients in the linear response theory, grounded on the coupling between the vector potential A and the wave number k as appeared in the cross term of the kinetic Hamiltonian $\frac{1}{2m^*}(\hbar k + eA)^2$ ($\hbar$ is the Planck constant and e is an electron charge).[11] Such response of the charge current to magnetic field is based on coherent electronic states described by k, being equivalent to phenomenological description of the Lorentz force subjected to spatially "continuous" current. Therefore, experimental observation of the Hall effect in hopping systems of localized charge significantly differs from what is expected for band-transport systems. Indeed, incoherent electronic systems such as amorphous silicon (a-Si) films show very small response to the application of magnetic field.[12–14]

At the present stage, the important remaining question is whether intermediate electronic states to bridge the self-localized polaron picture and diffusive bandlike transport can exist, and what the nature is of such electronic states if so. This study using Hall effects shows that pentacene OFETs, which are the most popular devices for expected practical use, appear to fit the missing link; the electronic carriers do couple magnetic field to provide finite Hall voltage, but the amount is considerably smaller than the band-transport value at room temperature. Intriguingly, the deviation of R_H from the band-transport value at near room temperature is almost

the same in the measured five samples, which include three single-crystal and two thin-film transistors. Since the Hall effect is the manifestation that the electrons couple to magnetic field through their plane-wave phase, one explanation for the result is that the one-electron phase coherence is weaker in pentacene layers than in the coherent band-transport systems, and that a new electronic state of the partially coherent electrons can be present in the OFETs. We also argue a possible origin of the partially coherent electrons based on the experimental results of temperature dependence of the Hall effect on the pentacene OFETs.

II. EXPERIMENT

We prepared both pentacene single-crystal and thin-film transistors for the Hall-effect measurement employing the Hall-bar structures. The pentacene single-crystal transistors were fabricated by the same method developed in our previous studies.[5,7] Highly doped Si was used for a gate electrode and a 500-nm-thick thermal oxide layer was used for a gate insulator with the unit-area capacitance C of 6.9 nF/cm^2. Source and drain electrodes were patterned by conventional photolithography, which consists of a 3-nm-thick Cr adhesion layer and a 17-nm-thick Au layer. The surface of the gate insulator was treated with self-assembled monolayers of heptadecafluorotriethoxysilane or decyltrichlorosilane before pentacene crystals were electrostatically laminated onto the surface. The crystals were grown by the physical vapor transport, using sublimed-grade powders of pentacene (Tokyo Chemical Industry Co., Ltd.) as a source. Sub-millimeter-size crystals were grown by further purification repeating the vaporizing processes at least twice before the final crystallization. For the thin-film transistors, thus, purified crystals were used to evaporate in vacuum onto decyltrichlorosilane-treated SiO_2/Si substrates at the deposition rate of 0.3 Å/sec. We form top-contact devices using evaporated Au electrodes to achieve sufficiently small contact resistances, which are essential to gain enough signal-to-noise ratio for the precise voltage measurements in the present Hall-effect measurements. In order to further reduce the contact resistances, we evaporate additional 2-nm-thick F_4-TCNQ layers on the pentacene films before the Au evaporation. Both the single-crystal and thin-film OFETs were carefully shaped to the "Hall bar" by using a laser-etching technique. Finally, the devices were encapsulated with 1000-nm-thick parylene film to ensure the stability of the device characteristics during the whole measurement.

Figure 1(a) shows an optical view of the pentacene single-crystal transistor and a schematic illustration of the measurement setup. Figure 1(b) is an optical view of a pentacene thin-film transistor where the channel dimensions are adjusted to almost the same values as in the single-crystal devices by a laser-etching technique. In Fig. 1(c), the atomic-force microscope (AFM) image of the thin-film device is exhibited, which indicates that pentacene covers whole the channel with the typical grains as large as a few μm.

In the Hall-effect measurements, voltages of V_1, V_2, and V_1' are measured at three different positions in the channel as illustrated in Fig. 1(a), so that four-terminal (sheet) conductivity $\sigma_\square = I/(V_2 - V_1) \cdot l/W$ and Hall voltage $V_H = V_1 - V_1'$

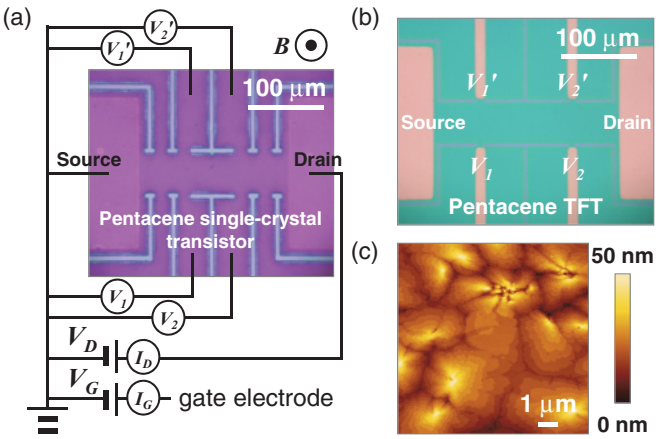

FIG. 1. (Color) (a) Optical view of a pentacene single-crystal transistor for the Hall-effect measurement. Schematic diagram is also shown for the measurement of voltages at different positions in the channel. The channel dimension of width W, length L, and distance l between voltage-probing electrodes are shaped to 60, 200, and 80 μm, respectively. (b) Optical view of a pentacene thin-film transistor for the Hall-effect measurement. (c) AFM image of a pentacene thin film.

are measured simultaneously as a function of gate voltage V_G. Here, $\sigma_\square$ equals the product of four-terminal field-effect mobility $\mu_{\rm FET}$ and charge density Q. Magnetic field is swept back and forth at least five times in the range from -10 to 10 T, so that slowly drifting signal is subtracted to evaluate ΔV_H for the peak-to-peak magnetic field and R_H is evaluated by $\Delta V_H/(I\Delta B)$, where $\Delta B = 20$ T.

III. RESULTS AND DISCUSSIONS

A. Device characteristics of the pentacene transistors

Figure 2 shows electrical characteristics of typical pentacene single-crystal and thin-film transistors at room temperature. Figure 2(a) exhibits sheet conductivity $\sigma_\square$ as a function of gate voltage in the linear regime for a pentacene single-crystal transistor. Both two-terminal conductivity $\sigma_{\square 2T} = I/V_D \cdot L/W$ and four-terminal conductivity $\sigma_{\square 4T} = I/(V_2^{(\prime)} - V_1^{(\prime)}) \cdot l/W$ are plotted together, where W, L, and l represent the channel width, length, and the distance between parallel voltage terminals for four-terminal measurement. Output characteristics of the same device are shown in Fig. 2(b). Figures 2(c) and 2(d) show electrical characteristics of a pentacene thin-film transistor. In both devices, $\sigma_{\square 2T}$ and $\sigma_{\square 4T}$ are almost identical, indicating that the contact resistances between the pentacene channels and the source and drain electrodes are both negligible as compared to the channel resistance at room temperature. In the output characteristics of Figs. 2(b) and 2(d), Ohmic characteristics in the low-V_D region show that charge injection at the contacts is satisfactory. Their well-saturated properties also indicate that nearly ideal pinch-off regions were successfully fabricated. The field-effect mobility $\mu_{\rm FET}$ was extracted by the four-terminal measurement using the equation $1/C \cdot \partial\sigma_{\square 4T}/\partial V_G$, so that the values were

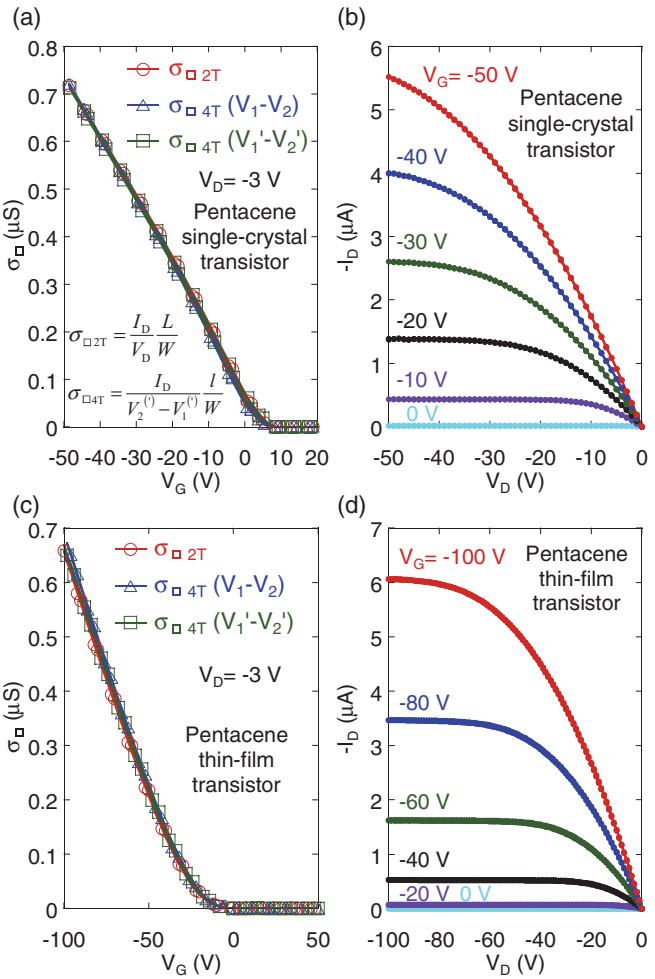

FIG. 2. (Color) (a) Sheet conductivity measured for typical pentacene single-crystal transistor. Both two-terminal conductivity (red circle plot) and four-terminal conductivity (blue triangle and green square plot) are plotted together. (b) Output characteristics measured for typical pentacene single-crystal transistor. (c), (d) Sheet conductivity and output characteristics measured for typical pentacene thin-film transistor.

estimated to be 2.0 and 1.5 cm^2/Vs for single-crystal and thin-film devices, respectively.

B. Hall effect in pentacene transistors

Figure 3 shows a typical Hall-effect profile measured for a pentacene single-crystal transistor at 280 K, where the transverse Hall voltages V_H at $V_G = -50$ V are plotted as a function of time with the drain voltage at -0.5 V. The Hall voltage slowly changes while ramping the magnetic field between 10 and -10 T, showing positive Hall coefficient, which is consistent with the positive charge carriers induced in the present measurement. The measurement accuracy of Hall voltages is improved compared to our previous reports[5,7,8] by refining the Hall-bar shape and increased device stability. As a result, the Hall voltages of sub-mV signals are detected with the measurement error of less than 10% at 280 K.

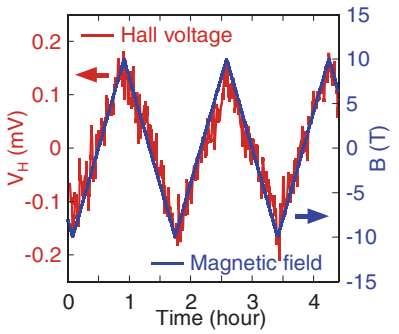

FIG. 3. (Color) Hall voltages (red line) measured as a function of time for a typical pentacene single-crystal transistor at fixed $V_D = -0.5$ V, $V_G = -50$ V, and $T = 280$ K. Ramping of the magnetic field between 10 and -10 T is shown by blue solid line.

Figures 4(a) and 4(b) show plots of the inverse Hall coefficient $1/R_H$ and $\sigma_\square$ as a function of V_G for the pentacene single-crystal device (single-crystal device 1) and the thin-film device (thin-film device 1) at 280 K, respectively. In both plots, $\sigma_\square$ increases with decreasing V_G due to the hole accumulation in the channel. Similarly, $1/R_H$ increases with decreasing V_G due to the charge accumulation, showing that the value of $1/R_H$ is proportional to the value of carrier density. The black broken line indicates the carrier density of Q calculated by the product of the capacitance C and the applied gate voltages $V_G - V_{\rm th}$, defining $V_{\rm th}$ by the threshold voltage derived from the extension of the slope of $1/R_H(V_G)$ to specify the threshold to induce well-mobile carriers disregarding trapped charge.

We note that the value of $1/R_H$ does not coincide with that of Q, but is twice as large as Q in the single-crystal device. The result is quantitatively reproducible in three single-crystal devices on substrates treated with different self-assembled monolayers. Similarly, the value of $1/R_H$ deviates from Q by the factor of 2 in thin-film devices, which is also consistent

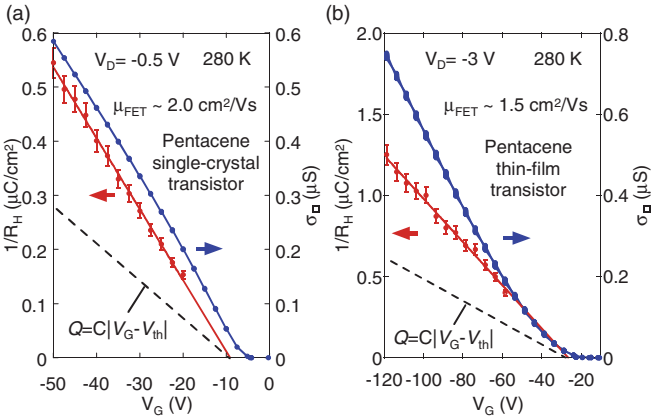

FIG. 4. (Color) (a), (b) Inverse Hall coefficient $1/R_H$ (red filled circles) and sheet conductivity (blue filled circles) plotted as a function of gate voltages at 280 K. The broken lines with the left-hand-side scale represent the carrier density estimated by the capacitance of the gate insulator and gate voltages. (a) and (b) are representing for a single-crystal device (single-crystal device 1) and a thin-film device (thin-film device 1), respectively.

with the results reported by Takamatsu *et al.*, considering the accuracy of the measurements.[15,16] Even as with the results of the same measurements for other thin-film devices with lower mobilities, the observation of twice as large $1/R_H(V_G)$ as Q is reproducible. Therefore, it is likely that the effect is attributed to intrinsic property of pentacene FETs rather than extrinsic effects such as grain boundaries. The results are already contrasting to those in previous measurements on rubrene and DNTT transistors, where the values of $1/R_H$ and Q precisely agree with each other and diffusive band-transport is realized.

C. Temperature dependence of the Hall effect

To further study the origin of the reduced Hall voltage in pentacene OFETs, we performed the measurement down to lower temperatures. Figure 5(a) shows temperature dependence of $\sigma_\square$ plotted as a function of V_G for the pentacene thin-film device 1. At a fixed V_G, $\sigma_\square$ decrease with decreasing temperature, partially because of decreasing carrier mobility $\mu_{\rm FET}$ and partially because of increasing $|V_{\rm th}|$ due to the increasing number of effective deep traps.[17] The inset of Fig. 5(a) shows the slope of $\sigma_\square(V_G)$ at high-V_G region for the same thin-film device 1, which corresponds to $\mu_{\rm FET}$ of well-mobile carriers. $\mu_{\rm FET}$ is almost constant in the high-temperature regime ($\geqslant$200 K), while the $\mu_{\rm FET}$ start to decrease with cooling below 200 K. The temperature profile of $\mu_{\rm FET}$ includes complex effects of shallow charge-trap levels, in which the effects are often simplified to the multiple trap-and-release model phenomenologically.

More importantly, Fig. 5(b) shows temperature-dependent $1/R_H$ as a function of V_G, in which the slope of $1/R_H(V_G)$ becomes less steep at lower temperatures. We note that the data are taken mostly at the high carrier concentration of 10^{12} cm^2, which contributes mostly to intrinsic well-mobile charge dynamics because of minimized effects of charge-localizing interface traps. Since the finite positive Hall voltage half as large as the normal band-transport value is detected in the pentacene transistors, its electronic state incorporates some degree of coherence over molecules. Although the phase coherence is weaker than that of the above ideal band-transport systems, the Hall voltage is generated by the presence of electromagnetic coupling between the external field (represented by the vector potential A) and wave vector k of the carriers induced at the surface of the pentacene semiconductors.

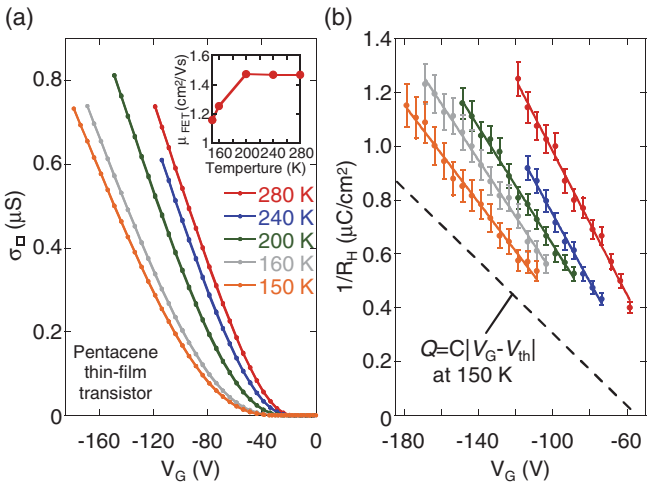

FIG. 5. (Color) (a) Temperature dependence of sheet conductivity as a function of gate voltage for a pentacene thin-film transistor (thin-film device 1). The inset shows the temperature dependence of the four-terminal field-effect mobility $\mu_{\rm FET}$. (b) Temperature dependence of inverse Hall coefficient plotted as a function of gate voltage for a pentacene thin-film transistor (thin-film device 1). The broken lines represent the carrier density estimated by the capacitance of the gate insulator and gate voltages.

As an example of a more incoherent electronic system, we note that disordered semiconductors such as a-Si typically show even smaller Hall voltage about one tenth of the band-transport value with sometimes anomalous sign.[12–14] In a microscopic model given by Friedman *et al.*, for example, the reduced Hall coefficient is reproduced by considering a "three-site interference" that describes electronic conduction dominated by disorder scattering. When the mean-free path approaches the atomic spacing, the carrier wave functions lack the phase coherence that would be present in the ordered lattices.[12] Dealing with elementary tunneling paths between the three atomic sites, the magnetic field penetrating the triangle connecting the three sites affects the electron-transfer integrals associated with these sites. As the result, finite Hall voltage appears but with much smaller values than when carriers propagate continuously to generate the full Lorentz force.

Also, it is argued in Ref. 14 that the finite Hall coefficient is measurable in even more disordered systems realized in heavily doped a-Si samples as the result of systematic experiments with various donor densities. As described by the percolation model with finite-length localized sites, this heavily doped regime is characterized by small (less than 0.01 cm^2/Vs even at room temperature) and rapidly diminishing Hall mobility μ_H with decreasing temperature. In contrast, the lightly doped "disorder-scattering" regime, which can be described in the Friedman model, shows temperature-independent μ_H typically as high as 0.1 cm^2/Vs. The inset of Fig. 6 shows temperature dependence of μ_H, which is experimentally given as $\mu_H \equiv R_H\sigma_\square$, for the present pentacene thin-film device 1. The temperature profile near room temperature at least

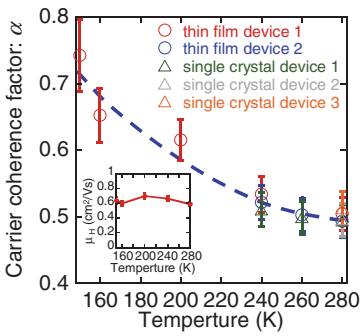

FIG. 6. (Color) Temperature dependence of α obtained in a variety of pentacene devices. The α is obtained by the formula $C/[\partial(1/R_H)/\partial V_G]$. The inset shows the temperature dependence of the Hall mobility μ_H for thin-film device 1, which is experimentally given as $\mu_H \equiv R_H\sigma_\square$.

qualitatively resembles the "disorder-scattering" case represented by the Friedman model. The idea of the microscopic charge coherence is at least describable with the microscopic interference between tunneling paths, although it significantly differs by considerably larger Hall coefficient and one order of magnitude larger value of the mobility.

For convenience, we introduce a factor α that describes the extent of the coupling between the partially extended electronic states and the external electromagnetic wave by the ratio of $1/R_H$ and Q. With the presence of finite $V_{\rm th}$, practical determination of α is given by $C/[\partial(1/R_H)/\partial V_G]$. α is exactly 1 for the previously measured free-electron-like OFETs. In addition, we note that α is larger than unity when the effect of shallow traps dominates the charge transport because $1/R_H$ measures only the well-mobile charge described with k. The situation resembles what was observed in the trap-dominated regime for rubrene single-crystal transistors at low temperature[6] and in the low-V_G region of DNTT thin-film transistors.[8] It is to be emphasized that the values of α are approximately 0.5 for two different samples of pentacene polycrystalline OFETs and three single-crystal samples with different mobilities. Therefore, the origin of the decoherence is intrinsic to the microscopic charge transport inside grains and not attributed to the trap states in grain boundaries. In addition, the nature of shallow traps is different from sample to sample, to which variety in carrier mobility among samples is usually attributed. Therefore, the universal value of α at room temperature suggests that the observation of the anomalous values of Hall coefficient is originated from fundamental charge state.

Figure 6 shows temperature dependence of α for all five pentacene devices. In all the measured samples, α elevates gradually with decreasing temperature, which possibly indicates that the value of R_H increases to approach the Hall coefficient of the band-transport model. Although it is generally difficult to retain sufficient signal-to-noise ratio for the measurement of small Hall voltage at low temperatures because of increasing contact impedance, the data are plotted for each sample down to the temperature where the measurement is still reproducible. Not only is the value at room temperature universal among the five samples, the temperature profile appears to be common within the accuracy of the measurement, which is consistent again to the idea that α describes the sample-independent intrinsic feature of the pentacene OFETs. Therefore, it is not likely that extrinsic contributions such as interface-trapping events predominantly govern the temperature profile of α. We note that the value of α increases already below 200 K upon cooling as shown in the red circles, whereas the value of mobility does not drop below 200 K as shown in the inset of Fig. 5(a), which would not happen if shallow interface traps really play the major role in the charge transport.

As a possible explanation of the observation, we propose the idea that fundamental electronic states regarding the extent of electronic phase coherence is significantly influenced by thermal effect in pentacene OFETs and that the dephasing effect is reduced at lower temperatures. Such thermally induced decoherence can be more pronounced than the conventional effect of electron-phonon scattering, where the picture of the band transport is preserved. Such assumption is recently addressed theoretically by Troisi *et al.* and by other groups,[18–21] where the influence of the molecular fluctuation is indeed very large, typically diminishing local transfer integral by half.[18]

The consideration can be also consistent with the report of temperature-dependent photoemission spectroscopy given by Koch *et al.*[22] in which the bandwidth of the holelike quasiparticles increases from 190 to 240 meV when the temperature is changed from room temperature down to 120 K. Furthermore, Sakanoue *et al.* reported significant enhancement in carrier mobility at very low temperature, where the authors attributed the observation to the molecular fluctuation.[4] Therefore, our present result may have demonstrated the fundamental electronic state as the incomplete phase coherence in weakly interacting clean molecular assembly. The mixing of the molecular orbitals causes some degree of the coherence against their spatial fluctuation, and such competition contributes the most intrinsic part in the charge transport for pentacene transistors, which is translated to the device performance of the best-studied organic semiconductor for industrial applications. Finally, we note that the phase-coherent factor α strongly differs by molecular species; α equals to unity and is temperature independent for previously studied rubrene and DNTT transistors.[7,8] For example, Troisi *et al.* suggested the possibility that the standard deviation of transfer integrals due to the molecular fluctuation increases with decreasing length of molecular π conjugation.[18] In addition, considering that transfer integrals are strongly affected by the molecular displacement,[23] we suspect that a sterically tangled molecular crystal such as a rubrene would be more advantageous against the thermal fluctuation due to their restricted motional freedom in the crystalline packing as compared to straight-rod pentacene. Further experimental and theoretical studies are expected to elucidate the microscopic origin that determines the extent of the molecular fluctuation.

IV. SUMMARY

To summarize, the precise measurement of Hall effects in single-crystal and thin-film transistors down to low temperatures tells us that fundamental electronic states consisted from the weakly coupled pentacene orbitals are significantly modulated with reduced coherence at room temperature. Given that the Hall effect is based on spatially extended electronic states described by wave functions, the extent of their phase coherence is experimentally deduced by α, which can indicate discrepancy from the band-transport model $\alpha = 1$. Since the value is universal to any thin-film or single-crystal pentacene OFETs, the electronic state appears to be intrinsic to microscopic charge dynamics unaffected by sample-dependent trap-level distributions. Intriguingly, the extent of the coherence is recovered at lower temperatures, which is understandable if we assume that molecular fluctuation significantly reduces the intermolecular electronic coupling. The mechanism of the observed thermally induced dephasing essentially impacts performance of organic transistors.

*uemura-t@sanken.osaka-u.ac.jp
†takeya@sanken.osaka-u.ac.jp

[1] M. Pope and C. Swenberg, *Electronic Processes in Organic Crystals and Polymers*, 2nd ed. (Oxford University Press, London, 1999), p. 374.
[2] K. Marumoto, N. Arai, H. Goto, M. Kijima, K. Murakami, Y. Tominari, J. Takeya, Y. Shimoi, H. Tanaka, S. I. Kuroda, T. Kaji, T. Nishikawa, T. Takenobu, and Y. Iwasa, Phys. Rev. B **83**, 075302 (2011).
[3] K. Marumoto, S. I. Kuroda, T. Takenobu, and Y. Iwasa, Phys. Rev. Lett. **97**, 256603 (2006).
[4] T. Sakanoue and H. Sirringhaus, Nat. Mater. **9**, 736 (2010).
[5] J. Takeya, K. Tsukagoshi, Y. Aoyagi, T. Takenobu, and Y. Iwasa, Jpn. J. Appl. Phys. **44**, L1393 (2005).
[6] V. Podzorov, E. Menard, J. A. Rogers, and M. E. Gershenson, Phys. Rev. Lett. **95**, 226601 (2005).
[7] J. Takeya, J. Kato, K. Hara, M. Yamagishi, R. Hirahara, K. Yamada, Y. Nakazawa, S. Ikehata, K. Tsukagoshi, Y. Aoyagi, T. Takenobu, and Y. Iwasa, Phys. Rev. Lett. **98**, 196804 (2007).
[8] M. Yamagishi, J. Soeda, T. Uemura, Y. Okada, Y. Takatsuki, T. Nishikawa, Y. Nakazawa, I. Doi, K. Takimiya, and J. Takeya, Phys. Rev. B **81**, 161306(R) (2010).
[9] Z. Q. Li, V. Podzorov, N. Sai, M. C. Martin, M. E. Gershenson, M. Di Ventra, and D. N. Basov, Phys. Rev. Lett. **99**, 016403 (2007).
[10] S. I. Machida, Y. Nakayama, S. Duhm, Q. Xin, A. Funakoshi, N. Ogawa, S. Kera, N. Ueno, and H. Ishii, Phys. Rev. Lett. **104**, 156401 (2010).
[11] See, e.g., H. Fukuyama, H. Ebisawa, and Y. Wada, Prog. Theor. Phys. **42**, 494 (1969).
[12] L. Friedman, J. Non-Cryst. Solids **6**, 329 (1971).
[13] E. Arnold and J. M. Shannon, Solid State Commun. **18**, 1153 (1976).
[14] P. G. LeComber, D. I. Jones, and W. E. Spear, Philos. Mag. **35**, 1173 (1977).
[15] T. Sekitani, Y. Takamatsu, S. Nakano, T. Sakurai, and T. Someya, Appl. Phys. Lett. **88**, 253508 (2006).
[16] Y. Takamatsu, T. Sekitani, and T. Someya, Appl. Phys. Lett. **90**, 133516 (2007).
[17] V. Podzorov, E. Menard, A. Borissov, V. Kiryukhin, J. A. Rogers, and M. E. Gershenson, Phys. Rev. Lett. **93**, 086602 (2004).
[18] A. Troisi, D. L. Cheung, and D. Andrienko, Phys. Rev. Lett. **102**, 116602 (2009).
[19] S. Fratini and S. Ciuchi, Phys. Rev. Lett. **103**, 266601 (2009).
[20] A. Troisi and G. Orlandi, J. Phys. Chem. A **110**, 4065 (2006).
[21] J. P. Sleigh, D. P. McMahon, and A. Troisi, Appl. Phys. A: Mater. Sci. Process. **95**, 147 (2009).
[22] N. Koch, A. Vollmer, I. Salzmann, B. Nickel, H. Weiss, and J. P. Rabe, Phys. Rev. Lett. **96**, 156803 (2006).
[23] D. A. DaSilva Filho, E.-G. Kim, and J.-L. Bredas, Adv. Mater. **17**, 1072 (2005).